

# RECENT CALCULATIONS OF ELECTROMAGNETIC AND STRONG DECAYS OF $N^*$

A. LEVIATAN<sup>a</sup> and R. BIJKER<sup>b</sup>

<sup>a</sup>*Racah Institute of Physics, The Hebrew University, Jerusalem 91904, Israel*

<sup>b</sup>*Instituto de Ciencias Nucleares, U.N.A.M., A.P. 70-543, 04510 México, D.F., México*

We report on recent calculations of electromagnetic elastic form factors, helicity amplitudes and strong decay widths of  $N^*$  resonances. The calculations are done in a collective constituent model for the nucleon, in which the resonances are interpreted as rotations and vibrations of an oblate top with a prescribed distribution of charges and magnetization.

## 1 Introduction

Effective models of baryons based on three constituents share a common spin-flavor-color structure but differ in their assumptions on the spatial dynamics. Quark potential models in nonrelativistic<sup>1</sup> or relativized<sup>2</sup> forms emphasize the single-particle aspects of quark dynamics for which only a few low-lying configurations in the confining potential contribute significantly to the eigenstates of the Hamiltonian. On the other hand, some regularities in the observed spectra (*e.g.* linear Regge trajectories, parity doubling) hint that an alternative, collective type of dynamics may play a role in the structure of baryons. In this contribution we present a particular collective model of baryons<sup>3</sup> and report on calculations of electromagnetic<sup>4</sup> and strong<sup>5</sup> couplings within this framework.

## 2 A Collective Model of Baryons

We consider a collective model in which the baryon resonances are interpreted in terms of rotations and vibrations of the string configuration in Fig. 1. The corresponding oblate top wave functions are spread over many oscillator shells and hence are truly collective. A typical mass spectrum in the collective model is shown in Fig. 2

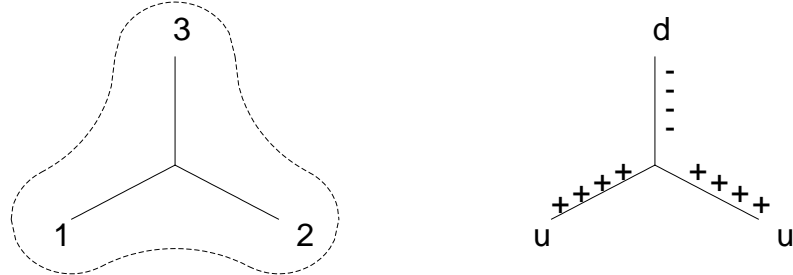


**Fig. 1.** Collective model of baryons (the charge distribution of the proton is shown as an example).

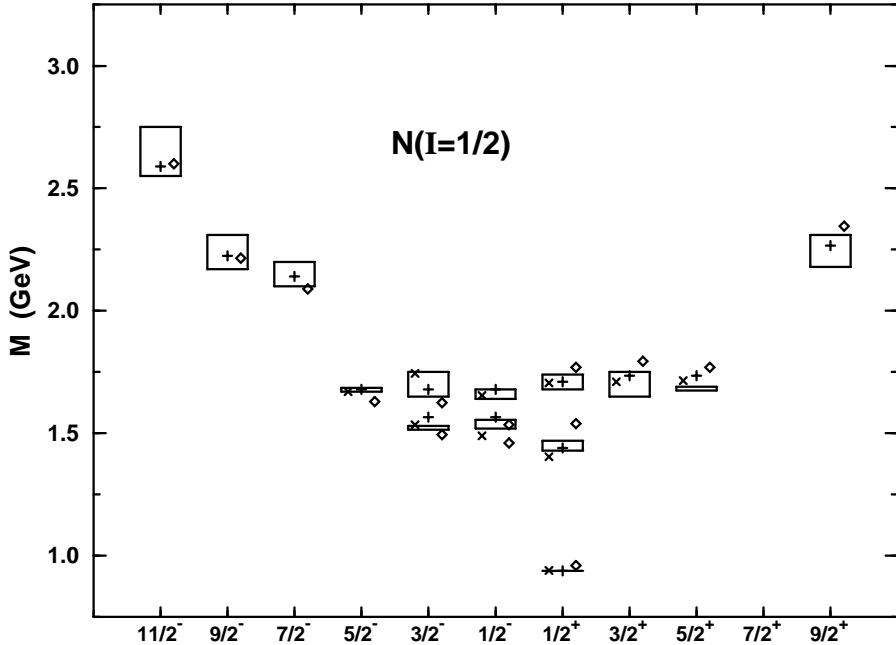


**Fig. 2.** Mass spectrum ( $M$  vs.  $J^P$ ) for  $3^*$  and  $4^*$  nucleon resonances. Collective model<sup>3</sup> (+), nonrelativistic quark model<sup>1</sup> ( $\times$ ), relativized quark model<sup>2</sup> ( $\diamond$ ).

along with a comparison to the non-relativistic<sup>1</sup> and relativized<sup>2</sup> quark models. As can be seen, the quality of the fits is comparable although the underlying dynamics is different. This shows that masses alone are not sufficient to distinguish between single-particle and collective forms of dynamics and one has to examine other observables which are more sensitive to the structure of wave-functions, such as electromagnetic and strong couplings.

To consider decay processes of baryon resonances in the collective model we need three ingredients. First, the wave functions of the initial and final states. These have the form

$$\left| {}^{2S+1} \dim \{SU_f(3)\}_J [\dim \{SU_{sf}(6)\}, L^P]_{(v_1, v_2); K} \right\rangle. \quad (1)$$

The spin-flavor part has the usual  $SU_{sf}(6)$  classification and determines the permutation symmetry of the state. The spatial part is characterized by the labels:  $(v_1, v_2); K, L^P$ , where  $(v_1, v_2)$  denotes the vibrations (stretching and bending) of the string configuration in Fig. 1;  $K$  denotes the projection of the rotational angular momentum  $L$  on the body-fixed symmetry-axis and  $P$  the parity. In this contribution we focus on the nucleon resonances of Fig. 1 which, with the exception of the  $N(1440)P_{11}$  and  $N(1710)P_{11}$  vibrational states, are associated with rotational excitations of the  $(v_1, v_2) = (0, 0)$  vibrational ground state. The second ingredient is the

form of the electromagnetic (strong) transition operator. It is assumed to involve the absorption or emission of a photon (elementary meson) from a single constituent. In such circumstances, the couplings discussed below can be expressed in terms of the operators

$$\begin{aligned}\hat{U} &= e^{-ik\sqrt{\frac{2}{3}}\lambda_z}, \\ \hat{T}_m &= \frac{im_3k_0}{2} \left( \sqrt{\frac{2}{3}}\lambda_m e^{-ik\sqrt{\frac{2}{3}}\lambda_z} + e^{-ik\sqrt{\frac{2}{3}}\lambda_z} \sqrt{\frac{2}{3}}\lambda_m \right),\end{aligned}\quad (2)$$

where  $\lambda_m$  ( $m = 0, \pm$ ) are Jacobi coordinates and  $(k_0, \vec{k})$  is the four-momentum of the absorbed quanta. The form factors of interest are proportional to the matrix elements of these operators in the wave-functions of Eq. (1). The third ingredient which specifies the collective model is the distribution of the charge and magnetization along the string. For the present analysis we use the (normalized) distribution

$$g(\beta) = \beta^2 e^{-\beta/a}/2a^3, \quad (3)$$

where  $\beta$  is a radial coordinate and  $a$  is a scale parameter. The collective form factors are obtained by folding the matrix elements of  $\hat{U}$  and  $\hat{T}_m$  with this probability distribution

$$\begin{aligned}\mathcal{F}(k) &= \int d\beta g(\beta) \langle \psi_f | \hat{U} | \psi_i \rangle, \\ \mathcal{G}_m(k) &= \int d\beta g(\beta) \langle \psi_f | \hat{T}_m | \psi_i \rangle.\end{aligned}\quad (4)$$

Here  $\psi$  denotes the spatial part of the baryon wave function. In Ref. [3] these form factors are evaluated algebraically and closed expressions can be derived in the limit of large model space. The ansatz of Eq. (3) for the probability distribution is made to obtain the dipole form for the elastic form factor. The same distribution is used to calculate inelastic form factors connecting other final states. All collective form factors are found<sup>4</sup> to drop as powers of  $k$ . This property is well-known experimentally and is in contrast with harmonic oscillator based quark models in which all form factors fall off exponentially.

### 3 Electromagnetic Form Factors and Helicity Amplitudes

The elastic electric ( $E$ ) and magnetic ( $M$ ) collective form factors are given by

$$\begin{aligned}G_E^N &= 3 \int d\beta g(\beta) \langle \Psi; M_J = 1/2 | e_3 \hat{U} | \Psi; M_J = 1/2 \rangle, \\ G_M^N &= 3 \int d\beta g(\beta) \langle \Psi; M_J = 1/2 | \mu_3 e_3 \sigma_{3,z} \hat{U} | \Psi; M_J = 1/2 \rangle,\end{aligned}\quad (5)$$

where  $\Psi$  denotes the nucleon wave function  $|{}^2S_{1/2}^N[56,0^+](0,0);0\rangle$  with  $N = p(n)$  for proton (neutron). Further  $e_3, \mu_3 = eg_3/2m_3, m_3, g_3, s_3 = \sigma_3/2$  are the charge (in units of  $e$ :  $e_u = 2/3, e_d = -1/3$ ), scale magnetic moment, mass,  $g$ -factor and spin, respectively, of the third constituent. Assuming  $SU_{sf}(6)$  spin-flavor symmetry ( $g_u = g_d, \mu_u = \mu_d$ ), we obtain the elastic electric form factors

$$G_E^p = \frac{1}{(1 + k^2 a^2)^2} ; \quad G_E^n = 0 , \quad (6)$$

and the magnetic form factors are proportional to  $G_E^p$  with a ratio  $G_M^n/G_M^p = -2/3$ . Within an effective model with three-constituents, in order to have a nonvanishing neutron electric form factor, as experimentally observed, one must break  $SU_{sf}(6)$ . This breaking can be achieved in various ways, *e.g.* by including in the mass operator a hyperfine interaction<sup>6</sup>, or by distorting the oblate-top geometry, allowing for a quark-diquark structure<sup>7</sup>. Within the model discussed here we study the breaking of the  $SU_{sf}(6)$  symmetry by assuming a flavor-dependent distribution

$$\begin{aligned} g_u(\beta) &= \beta^2 e^{-\beta/a_u}/2a_u^3 , \\ g_d(\beta) &= \beta^2 e^{-\beta/a_d}/2a_d^3 . \end{aligned} \quad (7)$$

In the calculations reported below we take  $g_u = g_d = 1$  and fix  $\mu_u$  and  $\mu_d$  from the measured magnetic moments. The scale parameters  $a_u$  and  $a_d$  in the distributions (7) are determined from a simultaneous fit to the proton and neutron charge radii, and to the proton and neutron electric and magnetic form factors. For the calculations in which the  $SU_{sf}(6)$  symmetry is satisfied this procedure yields  $a_u = a_d = a = 0.232$  fm and  $\mu_u = \mu_d = \mu_p = 2.793 \mu_N$  ( $= 0.126 \text{ GeV}^{-1}$ ). When  $SU_{sf}(6)$  symmetry is broken we find  $a_u = 0.230$  fm,  $a_d = 0.257$  fm,  $\mu_u = 2.777 \mu_N$  ( $= 0.126 \text{ GeV}^{-1}$ ) and  $\mu_d = 2.915 \mu_N$  ( $= 0.133 \text{ GeV}^{-1}$ ).

Fig. 3 shows the electric and magnetic form factors of the proton and the neutron. We see that while the breaking of spin-flavor symmetry can account for the non-zero value of  $G_E^n$  and gives a good description of the data, it worsens the fit to the proton electric and neutron magnetic form factors. This implies either that the simple mechanism for spin-flavor breaking of Eq. (7) does not produce the right phenomenology and other contributions, such as polarization of the neutron into  $p + \pi^-$ , play an important role in the neutron electric form factor<sup>8</sup>. (A coupling to the meson cloud through  $\rho, \omega$  and  $\phi$  mesons is indeed expected<sup>9</sup> to contribute in this range of  $Q^2$ .) This conclusion (*i.e.* worsening the proton form factors) applies also to the other mechanisms of spin-flavor symmetry breaking mentioned above, such as that induced by a hyperfine interaction<sup>6</sup> which gives  $a_u < a_d$  ('moves the up quark to the center and the down quark to the periphery'). This pattern is a consequence of the fact that within the framework of constituent models  $G_E^p, G_E^n, G_M^p$  and  $G_M^n$  are intertwined.

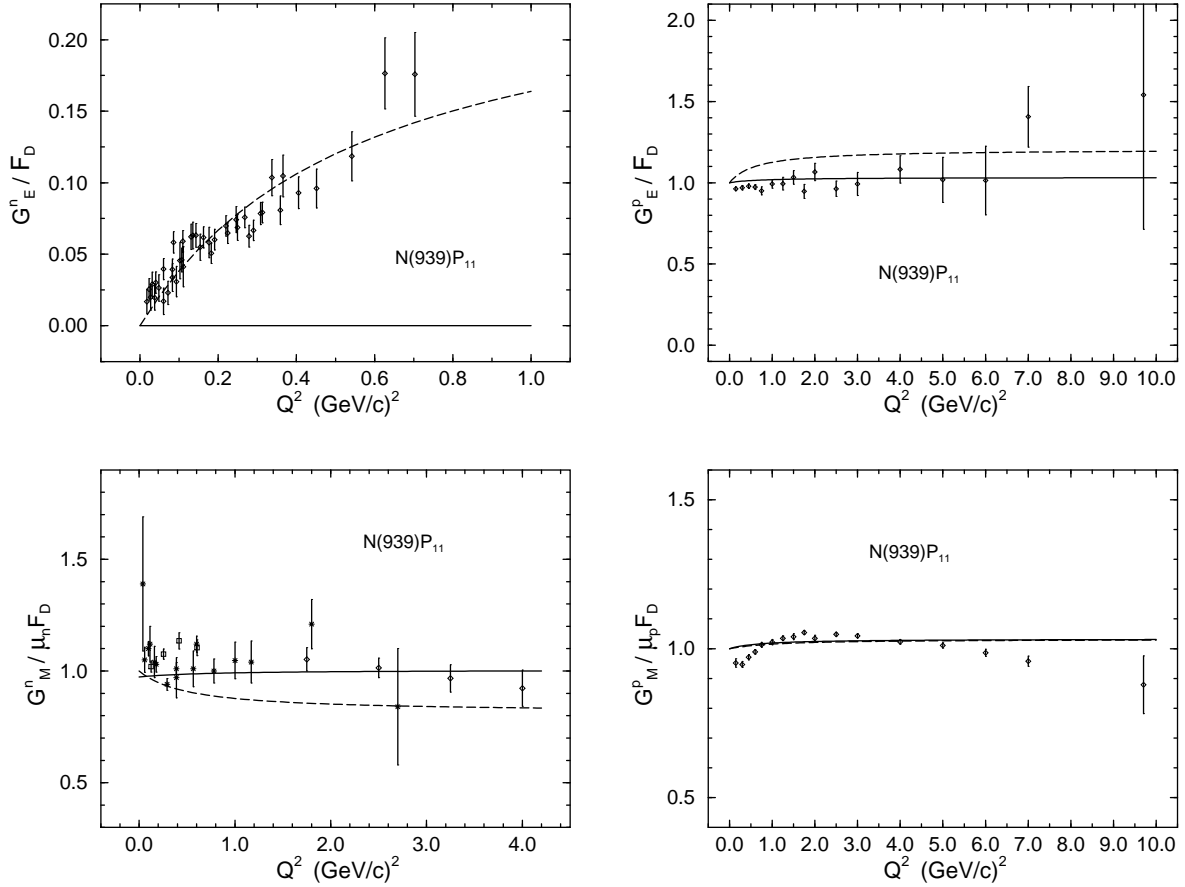


**Fig. 3.** Neutron and proton electric ( $G_E^n$ ,  $G_E^p$ ) and magnetic ( $G_M^n/\mu_n$ ,  $G_M^p/\mu_p$ ) form factors divided by  $F_D = 1/(1+Q^2/0.71)^2$ . Dashed (solid) lines correspond to a calculation with (without) flavor breaking.

Other (observable) quantities of interest are the helicity amplitudes in photo- and electroproduction. The transverse helicity amplitudes between the initial (ground) state of the nucleon and the final (excited) state of a baryon resonance are

$$A_\nu^N = 6\sqrt{\frac{\pi}{k_0}} \left[ k \langle L, 0; S, \nu | J, \nu \rangle \mathcal{B} - \langle L, 1; S, \nu - 1 | J, \nu \rangle \mathcal{A} \right], \quad (8)$$

where  $\nu = 1/2, 3/2$  indicates the helicity. The orbit- and spin-flip amplitudes ( $\mathcal{A}$  and  $\mathcal{B}$ , respectively) are given by

$$\begin{aligned} \mathcal{B} &= \int d\beta g(\beta) \langle \Psi_f; M_J = \nu | \mu_3 e_3 s_{3,+} \hat{U} | \Psi_i; M'_J = \nu - 1 \rangle, \\ \mathcal{A} &= \int d\beta g(\beta) \langle \Psi_f; M_J = \nu | \mu_3 e_3 \hat{T}_+ / g_3 | \Psi_i; M'_J = \nu - 1 \rangle. \end{aligned} \quad (9)$$

These observables correspond to an absorption process ( $\gamma + B' \rightarrow B$ ) of a right-handed

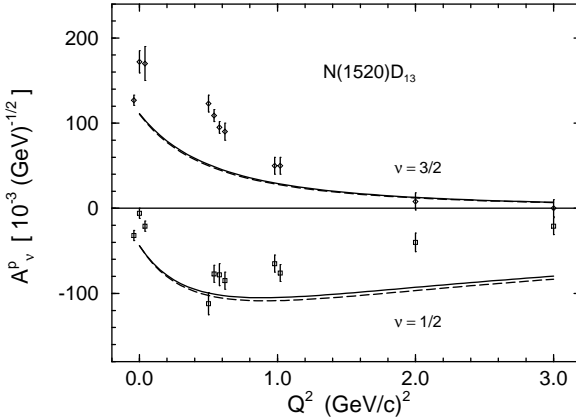


**Fig. 4.** Proton helicity amplitudes for excitation of  $N(1520)D_{13}$ . Notation for dashed (solid) lines as in Fig. 3

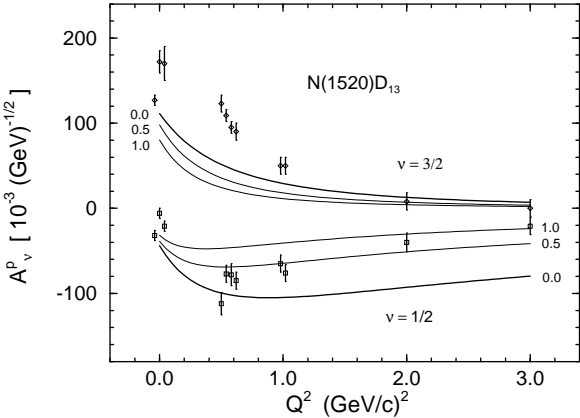


**Fig. 5.** Effect of hadron swelling for excitation of  $N(1520)D_{13}$ . The curves are labelled by the stretching parameter  $\xi$  of Eq. (10).

photon with four-momentum ( $k_0, \vec{k} = k\hat{z}$ ). In Eq. (9)  $|\Psi_i\rangle$  denotes the (space-spin-flavor) wave function of the initial nucleon ( $B'$ ) with  $|^{28}_{1/2}N[56, 0^+](0,0);0\rangle$  and  $N = p, n$ , and, similarly,  $|\Psi_f\rangle$  that of the final baryon resonance ( $B$ ). In general, the  $\mathcal{B}$  and  $\mathcal{A}$  amplitudes of Eq. (9) are proportional to the collective form factors  $\mathcal{F}$  and  $\mathcal{G}_+$  of Eq. (4), respectively. When spin-flavor symmetry is broken the helicity amplitudes are given in terms of flavor-dependent collective form factors  $\mathcal{F}_u(k)$ ,  $\mathcal{G}_{u,+}(k)$  and  $\mathcal{F}_d(k)$ ,  $\mathcal{G}_{d,+}(k)$ , which depend on the size parameters,  $a_u$  and  $a_d$ , respectively<sup>4</sup>.

The transverse helicity amplitudes  $A_{1/2}^p$ ,  $A_{3/2}^p$  in the Breit frame for  $N(1520)D_{13}$  are shown in Fig. 4 (a factor of  $+i$  is suppressed). As seen, the effect of spin-flavor breaking is rather small. Only in those cases in which the amplitude with  $SU_{sf}(6)$  symmetry is zero, the effect is of some relevance. Such is the case with proton helicity amplitudes for the  $^48_J[70, L^P]$  multiplet (*e.g.* the  $L^P = 1^-$  resonances  $N(1675)D_{15}$  and  $N(1700)D_{13}$ ) and with neutron  $\nu = 3/2$  amplitudes for the  $^28_J[56, L^P]$  multiplet (*e.g.* the  $L^P = 2^+$  resonance  $N(1680)F_{15}$ ).

In a string-like model of hadrons one expects<sup>10</sup> on the basis of QCD that strings will elongate (hadrons swell) as their energy increases. This effect can be easily included in the present analysis by making the scale parameters of the strings energy-dependent. We use here the simple ansatz

$$a = a_0 \left( 1 + \xi \frac{W - M}{M} \right), \quad (10)$$

where  $M$  is the nucleon mass and  $W$  the resonance mass. This ansatz introduces a new parameter ( $\xi$ ), the stretchability of the string. Fig. 5 shows that the effect of stretching on the helicity amplitudes for  $N(1520)D_{13}$  is rather large (especially if one takes the value  $\xi \approx 1$  which is suggested by QCD arguments<sup>10</sup> and the Regge behavior

of nucleon resonances). In particular, the data for  $N(1520)D_{13}$  (and  $N(1680)F_{15}$ ) show a clear indication that the form factors are dropping faster than expected on the basis of the dipole form.

## 4 Strong Decay Widths

In addition to electromagnetic couplings, strong decays of baryons provide an important, complementary, tool to study their structure. We consider strong decays of the form  $B \rightarrow B' + M$ . The process involves an emission (by one of the constituents in  $B$ ) of an elementary pseudoscalar meson meson ( $M = \pi$  or  $\eta$ ) with energy  $k_0 = E_M = E_B - E_{B'}$  and momentum  $\vec{k} = \vec{P}_M = \vec{P} - \vec{P}' = k\hat{z}$ . Here  $\vec{P}$  and  $\vec{P}'$  are the momenta of the initial ( $B$ ) and final baryon ( $B'$ ). The calculations are performed in the rest frame of  $B$  ( $P_z = 0$ ). For decays in which the initial baryon has angular momentum  $\vec{J} = \vec{L} + \vec{S}$  and in which the final baryon is either the nucleon or the delta, the (strong) helicity amplitudes in the collective model are

$$A_\nu(k) = \frac{1}{(2\pi)^{3/2}(2k_0)^{1/2}} \left[ \langle L, 0, S, \nu | J, \nu \rangle \zeta_0 Z_0(k) + \frac{1}{2} \langle L, 1, S, \nu - 1 | J, \nu \rangle \zeta_+ Z_-(k) + \frac{1}{2} \langle L, -1, S, \nu + 1 | J, \nu \rangle \zeta_- Z_+(k) \right]. \quad (11)$$

The coefficients  $\zeta_m$  ( $m = 0, \pm$ ) are spin-flavor matrix elements<sup>5</sup> and the  $Z_m(k)$  are radial matrix elements

$$\begin{aligned} Z_0(k) &= 6 \left[ gk - \frac{1}{6} hk \right] \mathcal{F}(k)^* - 6h \mathcal{G}_z(k)^*, \\ Z_\pm(k) &= -6h \mathcal{G}_\mp(k)^*, \end{aligned} \quad (12)$$

involving the same collective form factors  $\mathcal{F}(k)$ ,  $\mathcal{G}_\mp(k)$  discussed in Eq. (4). The coefficients  $g$  and  $h$  denote the strength of two terms in the transition operator. The decay widths for a specific channel are given by

$$\Gamma(B \rightarrow B' + M) = 2\pi\rho_f \frac{2}{2J + 1} \sum_{\nu > 0} |A_\nu(k)|^2. \quad (13)$$

where  $\rho_f$  is a phase space factor. In the algebraic method the widths can be obtained in closed form which allows us to do a straightforward and systematic analysis of the experimental data.

We consider here decays with emission of  $\pi$  and  $\eta$ . The experimental data<sup>11</sup> are shown in Tables 1 and 2, where they are compared with the results of our calculation. The calculated values depend on the two parameters  $g$  and  $h$  in Eq. (12) and on the scale parameter  $a$  of Eq. (3). In the present analysis we determine these parameters from a least square fit to the  $N\pi$  partial widths (which are relatively well known) with the exclusion of the  $S_{11}$  resonances. For the latter the situation is not clear due to

Table 1.  $N\pi$  decay widths of  $3^*$  and  $4^*$  nucleon resonances in MeV.

State	Mass	Resonance	$k$ (MeV)	$\Gamma$ (th)	$\Gamma$ (exp)
$S_{11}$	$N(1535)$	$^2S_{1/2}[70, 1^-]_{(0,0);1}$	467	85	$79 \pm 38$
$S_{11}$	$N(1650)$	$^4S_{1/2}[70, 1^-]_{(0,0);1}$	547	35	$130 \pm 27$
$P_{13}$	$N(1720)$	$^2S_{3/2}[56, 2^+]_{(0,0);0}$	594	31	$22 \pm 11$
$D_{13}$	$N(1520)$	$^2S_{3/2}[70, 1^-]_{(0,0);1}$	456	115	$67 \pm 9$
$D_{13}$	$N(1700)$	$^4S_{3/2}[70, 1^-]_{(0,0);1}$	580	5	$10 \pm 7$
$D_{15}$	$N(1675)$	$^4S_{5/2}[70, 1^-]_{(0,0);1}$	564	31	$72 \pm 12$
$F_{15}$	$N(1680)$	$^2S_{5/2}[56, 2^+]_{(0,0);0}$	567	41	$84 \pm 9$
$G_{17}$	$N(2190)$	$^2S_{7/2}[70, 3^-]_{(0,0);1}$	888	34	$67 \pm 27$
$G_{19}$	$N(2250)$	$^4S_{9/2}[70, 3^-]_{(0,0);1}$	923	7	$38 \pm 21$
$H_{19}$	$N(2220)$	$^2S_{9/2}[56, 4^+]_{(0,0);0}$	905	15	$65 \pm 28$
$I_{1,11}$	$N(2600)$	$^2S_{11/2}[70, 5^-]_{(0,0);1}$	1126	9	$49 \pm 20$

possible mixing of  $N(1535)S_{11}$  and  $N(1650)S_{11}$  and the possible existence of a third  $S_{11}$  resonance<sup>12</sup>. As a result we find  $g = 1.164 \text{ GeV}^{-1}$  and  $h = -0.094 \text{ GeV}^{-1}$ . The relative sign is consistent with a previous analysis of the strong decay of mesons<sup>13</sup> and with a derivation from the axial-vector coupling. The scale parameter,  $a = 0.232 \text{ fm}$ , extracted in the present fit is found to be equal to the value extracted in the calculation of electromagnetic couplings<sup>4</sup>. We keep  $g$ ,  $h$  and  $a$  equal for *all* resonances and *all* decay channels ( $N\pi$ ,  $N\eta$ ,  $\Delta\pi$ ,  $\Delta\eta$ ). In comparing with previous calculations, it should be noted that in the calculation in the nonrelativistic quark model<sup>14</sup> the decay widths are parametrized by four reduced partial wave amplitudes instead of the two elementary amplitudes  $g$  and  $h$ . Furthermore, the momentum dependence of these reduced amplitudes are represented by constants. The calculation in the relativized quark model<sup>15</sup> was done using a pair-creation model for the decay and involved a different assumption on the phase space factor. Both the nonrelativistic and relativized quark model calculations include the effects of mixing induced by the hyperfine interaction, which in the present calculation are not taken into account.

The calculation of decay widths of  $3^*$  and  $4^*$  nucleon resonances into the  $N\pi$  channel is found to be in fair agreement with experiment (see Table 1). The same holds for the  $\Delta\pi$  channel<sup>5</sup>. These results are to a large extent a consequence of spin-flavor symmetry. There does not seem to be anything unusual in the decays into  $\pi$  and our analysis confirms the results of previous analyses.

Contrary to the decays into  $\pi$ , the decay widths into  $\eta$  have some unusual properties. The calculation gives systematically small values for these widths (see Table 2). This is due to a combination of phase space factors and the structure of the transition

Table 2.  $N^* \rightarrow N\eta$  decay widths of (3\* and 4\*) nucleon resonances in MeV.

State	Mass	$k$ (MeV)	$\Gamma$ (th)	$\Gamma$ (exp)
$S_{11}$	$N(1535)$	182	0.1	$74 \pm 39$
$S_{11}$	$N(1650)$	346	8	$11 \pm 6$
$P_{13}$	$N(1720)$	420	0.2	
$D_{13}$	$N(1520)$	150	0.6	
$D_{13}$	$N(1700)$	400	4	
$D_{15}$	$N(1675)$	374	17	
$F_{15}$	$N(1680)$	379	0.5	
$G_{17}$	$N(2190)$	791	11	
$G_{19}$	$N(2250)$	831	9	
$H_{19}$	$N(2220)$	811	0.7	
$I_{1,11}$	$N(2600)$	1054	3	

operator. Due to the difference between the  $\pi$  and  $\eta$  mass, the  $\eta$  decay widths are suppressed relative to the  $\pi$  decays. The spin-flavor part is approximately the same for  $N\pi$  and  $N\eta$ , since  $\pi$  and  $\eta$  are in the same  $SU_f(3)$  multiplet. We emphasize here, that the transition operator was determined by fitting the coefficients  $g$  and  $h$  to the  $N\pi$  decays of the 3\* and 4\* resonances. Hence the  $\eta$  decays are calculated without introducing any further parameters.

The experimental situation is unclear. The 1992 PDG compilation gave systematically small widths ( $\sim 1$  MeV) for all resonances except  $N(1535)S_{11}$ . The 1994 PDG compilation deleted all  $\eta$  widths with the exception of  $N(1535)S_{11}$ . This situation persists in the latest PDG compilation<sup>11</sup>, where  $N(1650)S_{11}$  is now assigned a small but non-zero  $\eta$  width. The results of our analysis suggest that the large  $\eta$  width for the  $N(1535)S_{11}$  is not due to a conventional  $q^3$  state. One possible explanation is the presence of another state in the same mass region, *e.g.* a quasi-bound meson-baryon  $S$  wave resonance just below or above threshold, for example  $N\eta$ ,  $K\Sigma$  or  $K\Lambda$ <sup>16</sup>. Another possibility is an exotic configuration of four quarks and one antiquark ( $q^4\bar{q}$ ).

## 5 Summary and Conclusions

Within a collective model of the nucleon we have analyzed simultaneously elastic form factors and helicity amplitudes in photo- and electroproduction and strong decay widths. The logic of the method is that, by starting from the charge and magnetization distribution of the ground state (assuming a dipole form to the elastic form factor of the nucleon), one can obtain the transition form factors to the excited

states. In the ‘collective’ model, this procedure yields *a power dependence of all form factors* (elastic and inelastic) on  $Q^2$ . For electromagnetic couplings we find that, whereas the breaking of the spin-flavor symmetry hardly effects the helicity amplitudes, the stretching of hadrons does have a noticeable influence. The disagreement between experimental and theoretical elastic form factors and helicity amplitudes in the low- $Q^2$  region  $0 \leq Q^2 \leq 1$  ( $\text{GeV}/c$ ) $^2$  may be due to coupling of the photon to the meson cloud, *i.e.* configurations of the type  $q^3 - q\bar{q}$ . Since such configurations have much larger spatial extent than  $q^3$ , their effects are expected to drop faster with momentum transfer  $Q^2$  than the constituent form factors. Within the same collective model we have performed a calculation of the strong widths for decays into  $\pi$  and  $\eta$ . The analysis of experimental data shows that, while the decays into  $\pi$  follow the expected pattern, the decays into  $\eta$  have some unusual features. Our calculations do not show any indication for a large  $\eta$  width, as is observed for the  $N(1535)S_{11}$  resonance. The observed large  $\eta$  width indicates the presence of another configuration, which is outside the present model space. Work on the extension of the formalism to include strange baryons is in progress.

The results reported in this article are based on work done in collaboration with F. Iachello (Yale). The work is supported in part by grant No. 94-00059 from the United States-Israel Binational Science Foundation (BSF), Jerusalem, Israel (A.L.) and by CONACyT, México under project 400340-5-3401E and DGAPA-UNAM under project IN105194 (R.B.).

1. N. Isgur and G. Karl, Phys. Rev. **D18**, 4187 (1978); **D19**, 2653 (1979); **D20**, 1191 (1979).
2. S. Capstick and N. Isgur, Phys. Rev. **D34**, 2809 (1986).
3. R. Bijker, F. Iachello and A. Leviatan, Ann. Phys. (N.Y.) **236**, 69 (1994).
4. R. Bijker, F. Iachello and A. Leviatan, Phys. Rev. **C54**, 1935 (1996).
5. R. Bijker, F. Iachello and A. Leviatan, nucl-th/9608057, Phys. Rev. **D**, in press.
6. N. Isgur, G. Karl and D.W.L. Sprung, Phys. Rev. **D23**, 163 (1981).
7. Y. Tzeng and S.S. Hsiao, Il Nuovo Cimento **106**, 573 (1993).
8. F.E. Close and R.R. Hogan, Nucl. Phys. **B185**, 333 (1981).
9. F. Iachello, A.D. Jackson and A. Lande, Phys. Lett. **B43**, 191 (1973).
10. K. Johnson and C.B. Thorn, Phys. Rev. **D13**, 1934 (1974); I. Bars and H.J. Hanson, Phys. Rev. **D13**, 1744 (1974).
11. Particle Data Group, Phys. Rev. **D54**, 1 (1996).
12. Z. Li and R. Workman, Phys. Rev. **C53**, R549 (1996).
13. C. Gobbi, F. Iachello and D. Kusnezov, Phys. Rev. **D50**, 2048 (1994).
14. R. Koniuk and N. Isgur, Phys. Rev. Lett. **44**, 845 (1980); Phys. Rev. **D21**, 1868 (1980).
15. S. Capstick and W. Roberts, Phys. Rev. **D47**, 1994 (1993); **D49**, 4570 (1994).
16. N. Kaiser, P.B. Siegel and W. Weise, Phys. Lett. **B362**, 23 (1995).